Heliyon 9 (2023) e13523

Contents lists available at ScienceDirect

Heliyon

journal homepage: www.cell.com/heliyon

Research article

Ni -chitosan/carbon nanotube: An efficient biopolymer -inorganic catalyst for selective hydrogenation of acetylene

Siye Tang [a,*], Liying Li [b], Xinxiang Cao [a,**], Qingqing Yang [a]

[a] College of Chemistry and Chemical Engineering, Luoyang Normal University, Luoyang 471934, China
[b] Henan Pingmei Shenma Dongda Chemistry Co., Ltd, Kaifeng 475003, China

ARTICLE INFO

Keywords:
Acetylene hydrogenation
Chitosan
Conversion
Heterogeneous catalysis
Nickel

ABSTRACT

This work developed an efficient Ni catalyst based on chitosan for selective hydrogenation of acetylene. The Ni catalyst was prepared by the reaction of the chitosan/carbon nanotube composite with $NiSO_4$ solution. The synthesized Ni-chitosan/carbon nanotube catalyst was characterized by inductively coupled plasma, FTIR, SEM and XRD. The results of FTIR and XRD demonstrated that Ni^{2+} successfully coordinated with chitosan. The addition of chitosan greatly improved the catalytic performances of Ni-chitosan/carbon nanotube catalyst. Over the Ni-chitosan/carbon nanotube catalyst, both the acetylene conversion and the selectivity to ethylene all achieved 100% at 160 °C and 190 °C, respectively. The catalytic performances of 6 mg Ni-chitosan/carbon nanotube catalyst were even better than that of 400 mg Ni single atom catalyst in literature. Extending the crosslinking time of chitosan and increasing the amount of the crosslinking agent were beneficial to enhance the catalytic effect of Ni-chitosan/carbon nanotube catalyst.

1. Introduction

Ethylene is an important basic feed in organic chemistry engineering, mainly used to produce polyethylene, polyvinyl chloride. A significant proportion of ethylene is produced from naphtha cracking [1]. This process makes ethylene to be contaminated with 0.5–2% of acetylene, which can poison the Ziegler-Natta catalysts used for downstream ethylene polymerization [2]. Selective hydrogenation of acetylene is always employed in industry to remove the trace acetylene to an acceptable level (<5 ppm) [3,4]. Namely, acetylene is effectively removed from ethylene-rich streams via selective hydrogenation to ethylene. At the same time, substantial hydrogenation of ethylene and over-hydrogenation of acetylene to undesirable ethane are avoided. So it is necessary to seek the catalysts with both high activity for acetylene conversion and high selectivity for ethylene. The traditional industrial catalysts are supported Pd-based systems, which are precious and usually show an excellent activity but a poor selectivity [5]. As non-precious metal, Ni has an absolute advantage in cost and Ni-based catalysts have been applied to selective hydrogenation of acetylene [4]. Ni-based catalysts used in the literature were usually separate Ni or mixture of Ni and other metals, such as Ni^{2+} confined in zeolite [6], Ni–Zn alloy on the $MgAl_2O_4$ spinel support [7,8], Cu-Ni-Fe [9], Cu–Ni/SiO_2 [10], NiCuMgAl-mixed metal oxides [11], Au–Ni/γ-Al_2O_3 [12], IB metal alloyed Ni [13,14], Ag–Ni/SiO_2 and Au–Ni/SiO_2 [15,16]. Nevertheless, the activity and selectivity towards selective hydrogenation of acetylene still require enhancement and the searching for low-cost substitutes is highly desired.

* Corresponding author.
** Corresponding author.
E-mail addresses: tsy6611@163.com (S. Tang), xiangzi827@163.com (X. Cao).

https://doi.org/10.1016/j.heliyon.2023.e13523
Received 5 October 2022; Received in revised form 24 January 2023; Accepted 2 February 2023
Available online 8 February 2023

Biomaterial supported catalysts have attracted much attention in last 20 years due to their eco-friendliness, non-toxicity, low-cost, bio-degradable features, and high metal adsorption capacity [17,18]. Chitin is the second most abundant biopolymer in nature after cellulose. Chitosan (CS) is the most important derivative of chitin and widely used in different areas such as waste water treatment, radioactive element and textile waste removal, medicine, agriculture, biotechnology, and food and pharmaceutical industries [17,19]. CS exhibits high affinity for metal ions due to the NH_2 and OH groups on its chains [20,21]. These functional groups can also make CS act as the ligand for transition metal ions [22]. CS has been an excellent candidate for building heterogeneous catalysts due to these attractive features and has served as a valuable support for several types of organocatalysts for different organic transformations [23]. CS can also stabilize the catalytic centers by preventing both the formation of aggregates (enhancement of the dispersion of nanoparticles) and the leaching of metal [24].

Nevertheless, to the best of our knowledge, there was no report on Ni-CS catalyst in the selective hydrogenation of acetylene by far. Herein, Ni-CS catalyst was synthesized and applied to the selective hydrogenation of acetylene. The synthesized Ni catalyst was characterized by inductively coupled plasma (ICP), Fourier transform infrared spectra (FTIR), scanning electron microscopy (SEM) and X-ray powder diffractometer (XRD). The results in this work will provide a new perspective for the further study of the Ni-based catalysts for selective hydrogenation reactions.

2. Experimental section

2.1. Materials

CS (pharmaceutical grade, 80–95% deacetylated) was purchased from Sinopharm Chemical Reagent Co., Ltd. (Shanghai, China). Multi-walled carbon nanotube (CNT) (98% (w/w), inradium: 2–5 nm, length: 10–30 μm, specific surface area: 200–300 m^2/g) was purchased from Guizhou Walls Technology Co., Ltd (Guizhou, China). All the other reagents were purchased from Tianjin Fuyu Fine Chemical Co., Ltd (Tianjin, China). They were of analytical grade and were used without further purification.

2.2. Preparation of the CS-CNT composite

0.1g of CS was put into a 250 mL round bottom flask. 50 mL of 2% (w/w) acetic acid aqueous solution was added to the flask. The suspension was then magnetically stirred at room temperature until the CS was completely dissolved. Then 0.1g of pristine CNT was put into the solution. The solution was sonicated in the ultrasonic cleaning pool (KQ-250DE, Kunshan Ultrasonic Instrument Co., Ltd, Jiangsu, China) for 4 h.

After sonication, the pH value of the solution was adjusted to pH = 8 with 5% (w/w) ammonia water. 0.5 mL of glutaraldehyde was used as the crosslinker and added to the above solution. The cross-linking reaction was performed at 55 °C for 2 h. The product was washed three times with deionized water and separated by centrifugation. Then the product was dried at 85 °C for 12 h. Changing the amount of cross-linking agent and cross-linking time, the corresponding CS-CNT samples were obtained.

2.3. Preparation of Ni-CS/CNT catalyst

0.1g of CS-CNT was put into a 100 mL round bottom flask. 10 mL of $NiSO_4$ aqueous solution with certain concentration was added to the flask. The mixed solution was magnetically stirred at room temperature for 2h. The product was treated and dried in term of the above method.

For comparison, the corresponding Ni-CS/CNT catalysts were prepared using $NiSO_4$ aqueous solutions with different molar concentrations. Meanwhile, Ni/CNT sample was also prepared using CNT instead of CS-CNT.

2.4. Characterization

By means of a mass spectrometry with ICP (ICAP6300 MFC, USA), the content of Ni in the prepared catalysts was measured. The structure of samples was investigated by FTIR (IR Spirit-T, Japan) using KBr disk technique. Each spectrum of the samples was acquired by accumulation of 45 scans with a resolution of 4 cm^{-1}. Morphology of all samples was characterized by SEM (Zeiss Sigma 500, Germany). The compositions' phases of the as-prepared materials were identified by a XRD (SmartLab SE, Japan) equipped with Cu Kα radiation (λ = 1.5418 Å) and operated at 40 kV and 40 mA with a 5°/min scan rate. The scanning angular range of 2 θ was performed from 5° to 90°.

2.5. Catalytic tests

All the activity tests were carried out in a tube quartz reactor (4 mm inner diameter) fixed in an oven with low temperature programmed capability. Prior to the start of each experimental run, 6 mg catalysts which were diluted with quartz sand to dissipate the heat were reduced in situ for 2 h under a flow of H_2/Ar mixture at 350 °C by heating from room temperature using a heating rate of 5 °C/min.

Then the reactor was cooled down to the reaction temperature under the protection of argon. A gas mixture of 20.00% (v/v) H_2, 19.05% (v/v) C_2H_4, 60.00% (v/v) Ar and 0.95% (v/v) C_2H_2 was introduced, the total flow rate of gas mixture was 30 mL/min. The volume ratio of H_2 and C_2H_2 was 21:1, the total gas hourly space velocity (GHSV) was 300000 mL/(h·g). All gas flows in the reaction

were controlled with mass flow controllers. The gas products from the reactor outlet were analyzed three times at each reaction temperature by an online gas chromatography (GC-2020, Tengzhou Zhongke Spectrum Analysis Instrument Co. Ltd, Shandong, China) equipped with a flame ionization detector.

The analysis data was collected using a PC work-station. Acetylene conversion and selectivity to ethylene were calculated using Eqs. (1) and (2):

$$C_2H_2 conversion = \frac{C_2H_2(in\ feed) - C_2H_2(in\ products)}{C_2H_2(in\ feed)} \times 100\% \quad (1)$$

$$C_2H_4 selectivity = \left(1 - \frac{C_2H_6(in\ products) - C_2H_6(in\ feed)}{C_2H_2(in\ feed) - C_2H_2(in\ products)} \times 100\%\right) \quad (2)$$

3. Results and discussion

3.1. ICP analysis

Actual loading of Ni analyzed by ICP were summarized in Table 1. From Table 1, the actual loading of Ni increased with the increase of $NiSO_4$ concentration. The Ni loading in Ni-CS/CNT is obviously greater than that in Ni/CNT when the concentration of $NiSO_4$ solution is 0.04 M. The reason should be that CS is able to adsorb more Ni.

The infrared spectra of CNT and Ni/CNT prepared using 0.04 M $NiSO_4$ were shown in Fig. 1. It can be seen that the infrared spectra of them have no change. This suggests that Ni particles were attached to CNT by physical adsorption.

The infrared spectra of CS, CNT and Ni-CS/CNT prepared using 0.04 M $NiSO_4$ were displayed in Fig. 2. Comparing with CS (Fig. 2(a)) and CNT (Fig. 2(b)), the infrared spectrum of Ni-CS/CNT varied significantly. In the spectrum of CS (Fig. 2(a)), the following characteristic peaks were observed: 1079.59 (C–O asymmetric stretching vibration), 1325.20 (C–N amino groups axial deformation), 1369.47 (C–O stretching vibration), 1422.31 (C–O stretching), 1660.79 (C═O stretching vibration), 2874.61 (C–H stretching vibration) and 3305.87 cm^{-1} (N–H symmetric stretching) [20,24–28]. The CS characteristic peaks located at 1079.59, 1325.20, 1422.31, 2874.61 as well as 3305.87 cm^{-1} disappeared or almost disappeared in Ni-CS/CNT spectrum (Fig. 2(c)). And characteristic bands at 1369.47, 1660.79 slightly decreased in intensity and shifted to 1355.19 cm^{-1}, 1600.81 cm^{-1}, respectively. In Ni-CS/CNT spectrum (Fig. 2(c)), the CNT characteristic bands at 1079.59, 1593.67 and 3447.25 cm^{-1} shifted to 1071.02 cm^{-1}, 1600.81 cm^{-1} and 3425.83 cm^{-1}, respectively. This result indicated the strong interaction between Ni^{2+} and CS. Accordingly, Ni^{2+} successfully coordinated with CS.

Furthermore, the effects of the crosslinking time and the amount of crosslinker on FTIR spectrum of Ni-CS/CNT were also analyzed. The results showed that the crosslinking time and the amount of the crosslinker did not affect the infrared spectrum of the Ni-CS/CNT catalyst.

The SEM images of Ni/CNT and Ni-CS/CNT prepared using 0.04 M $NiSO_4$ are shown in Fig. 3. Comparing Fig. 3(a) with Fig. 3(b), it can be seen that CS was membranous and covered the CNT surface. This proved that Ni which coordinated with CS was on the surface of the Ni-CS/CNT catalyst. The active Ni was anchored on the surface of the Ni-CS/CNT catalyst greatly improved the catalytic effect. Since only the Ni on the surface could serve as the active sites, while Ni inside the catalyst was the spectator which leaded to a waste of Ni [29].

As shown in Fig. 4, two peaks at $2\theta = 25.68^\circ$ and 43.00° were observed in the XRD pattern of CNT. In the pattern of Ni/CNT prepared using 0.04 M $NiSO_4$, the strong peaks at $2\theta = 25.52^\circ$ and 43.00° were attributed to the plane of CNT. However, no peak of Ni species was observed. The reason should be that the content of Ni species (1.43% (w/w) actual load) was well below the detection limit [30,31]. For the Ni-CS/CNT prepared using 0.04 M $NiSO_4$ catalyst, there were three peaks at $2\theta = 19.96^\circ$, 25.52° and 42.84°. The first peak of 19.96° was assigned to the plane of the chitosan structure [25,28,32]. The latter two peaks were attributed to CNT. The diffraction peaks of the Ni-CS/CNT changed significantly in comparison with CNT and Ni/CNT. This indicated that the obvious chemical interaction between CS and Ni existed, that is, CS had coordinated with Ni.

The catalytic performances on Ni-CS/CNT and Ni/CNT obtained by using 0.04 M $NiSO_4$ were tested, the results were shown in Fig. 5(a), (b) and (c).

The acetylene conversion over Ni-CS/CNT and Ni/CNT was shown in Fig. 5(a). It can be seen that the conversion enhanced as the temperature increased. When temperature was below 120 °C, the conversion on Ni/CNT was slightly higher than that of Ni-CS/CNT. Both conversions were almost equal at 120 °C. At 120 °C, the values of conversion on Ni-CS/CNT and Ni/CNT were 30.0% and 28.0%, respectively. When temperature was above 120 °C, the conversion on Ni-CS/CNT was much higher than that of Ni/CNT. The acetylene

Table 1
Actual loading of Ni in catalysts.

Sample	Actual loading (% w/w)	Concentration of $NiSO_4$ solution (M)
Ni-CS/CNT	1.18	0.03
Ni-CS/CNT	1.43	0.04
Ni-CS/CNT	1.95	0.06
Ni-CS/CNT	2.10	0.07
Ni/CNT	0.06	0.04

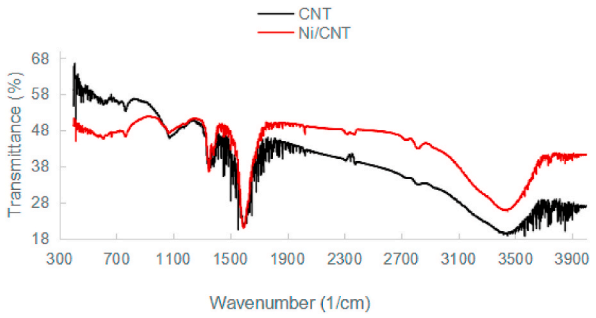

Fig. 1. FTIR spectra of CNT and Ni/CNT.

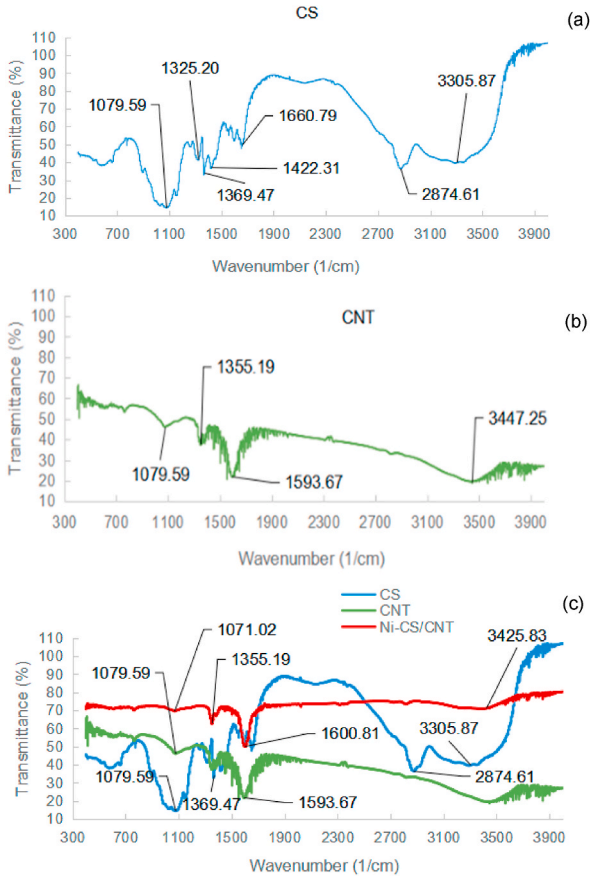

Fig. 2. FTIR spectra of CS (a), CNT (b) and Ni-CS/CNT (c).

conversion over Ni-CS/CNT could achieve 100% at 160 °C. However, the acetylene conversion over Ni/CNT reached the maximum 58.0% at 190 °C. The conversion on Ni-CS/CNT was obviously higher than that on Ni/CNT at the same temperature.

Fig. 5(b) showed the selectivity change with temperature. It can be seen that the selectivity on Ni/CNT increased with the increasing temperature. The selectivity on Ni-CS/CNT basically decreased with the increasing temperature before 170 °C, then rose sharply from 170 °C and reached 100% at 190 °C. From Fig. 5(a) and (b), the acetylene conversion and the selectivity to ethylene over Ni-CS/CNT catalyst were all 100% at 190 °C.

The relationship between selectivity and conversion over Ni-CS/CNT and Ni/CNT was presented in Fig. 5(c). It can be seen that the selectivity of Ni-CS/CNT was higher than that of Ni/CNT at the same conversion. Obviously, addition of CS provided higher catalytic performance. This was due to that the coordination of CS with Ni enhanced the dispersion of Ni in Ni-CS/CNT. Therefore, the Ni-CS/CNT catalyst was more conducive to the acetylene selective hydrogenation reaction than Ni/CNT.

Under the same volume ratio of H_2 and C_2H_2, the conversion and selectivity of Ni-CS/CNT catalyst prepared in this work even outperformed the Ni single atom catalyst which is well known as an excellent catalyst now. X. Y. Dai et al. synthesized Ni single atom

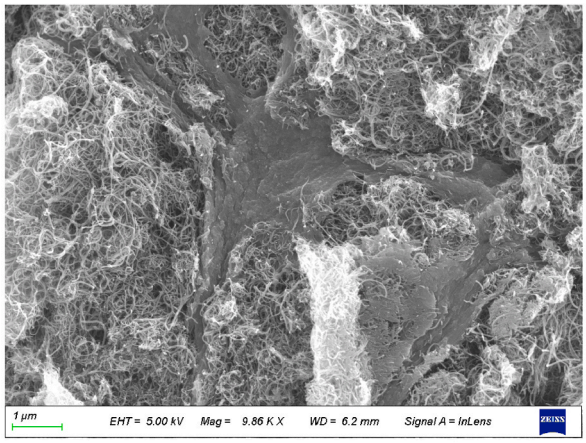

(a)

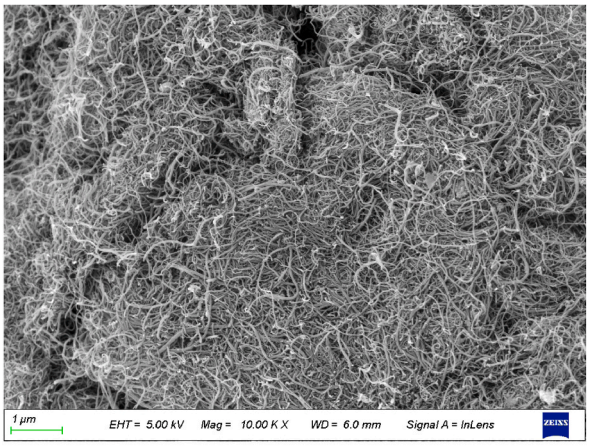

(b)

Fig. 3. SEM pictures of Ni-CS/CNT (a) and Ni/CNT (b).

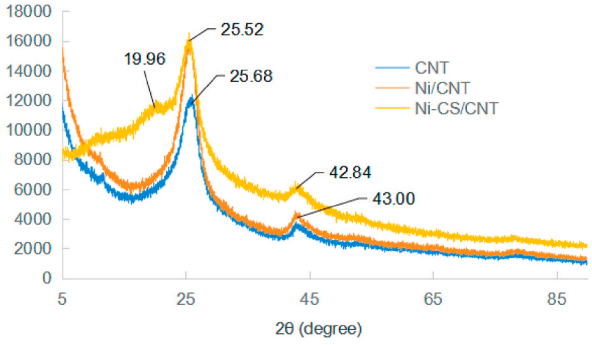

Fig. 4. XRD patterns of CNT, Ni/CNT and Ni-CS/CNT.

supported on N-doped carbon (Ni SAs/N–C) through a pyrolysis process, during which the aggregation of Ni atoms were strictly limited by carbon frameworks [3]. Up to 200 °C, the conversion and selectivity of the Ni single atom catalyst were only 95% and 91%, respectively. In addition, the amount of catalyst strongly confirmed that the catalytic performances of Ni-CS/CNT catalyst obtained in this work were better than that of Ni single atom catalyst synthesized by X. Y. Dai et al. We only used 6 mg Ni-CS/CNT catalyst, while X. Y. Dai et al. used 400 mg Ni single atom catalyst [3].

Effect of concentration of $NiSO_4$ solution on the catalytic performances.

Acetylene hydrogenation reaction was carried out on the Ni-CS/CNT catalyst using different concentrations of $NiSO_4$. The results

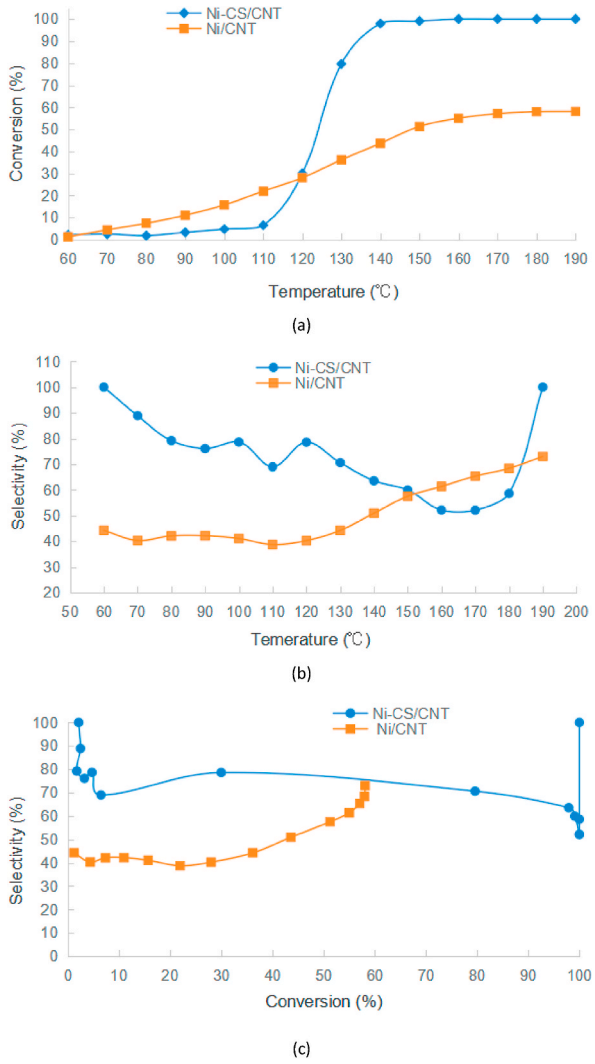

Fig. 5. Acetylene conversion (a), ethylene selectivity (b) and the relationship between ethylene selectivity and acetylene conversion (c) of Ni-CS/CNT and Ni/CNT.

were shown in Fig. 6. From Fig. 6(a), it can be seen that the conversion enhanced as the temperature increased. Acetylene could fully transformed on these catalysts prepared using different concentrations of $NiSO_4$. The temperatures of complete conversion were 0.03 M: 130 °C, 0.04 M: 160 °C, 0.06 M: 190 °C and 0.07 M: 140 °C, respectively.

The relationship between selectivity and conversion over Ni-CS/CNT was presented in Fig. 6(b). The Ni-CS/CNT catalyst prepared using 0.04 M $NiSO_4$ had higher selectivity at the same conversion. Therefore, 0.04 M was chosen as the optimal concentration of $NiSO_4$ solution.

Effect of CS-CNT crosslinking time on the catalytic performances.

Taking 0.06 M $NiSO_4$ for example, the catalytic performances of the Ni-CS/CNT catalysts obtained at different crosslinking times were shown in Fig. 7.

As can be seen from Fig. 7(a), the conversion of the Ni-CS/CNT catalysts prepared at different crosslinking times increased as the reaction temperature increased. The conversion of the Ni-CS/CNT catalyst prepared by crosslinking for 4 h could achieve 100% at 150 °C, while the Ni-CS/CNT catalyst prepared by crosslinking for 2 h reached 100% acetylene conversion until 190 °C.

Fig. 7(b) shows that the selectivity of the Ni-CS/CNT catalyst prepared by crosslinking for 4 h was very excellent and was all 100% over the entire temperature range. The Ni-CS/CNT catalyst prepared by crosslinking for 2 h also showed excellent selectivity of 100% from 60 to 90 °C. However, the selectivity maintained 45%–80% above 90 °C. It is clear that extending crosslinking time was beneficial to improve the catalytic effect.

Taking 0.06 M $NiSO_4$ for example, the catalytic performances of the Ni-CS/CNT catalysts prepared using different glutaraldehyde dosages were shown in Fig. 8.

From Fig. 8(a), the conversion gradually increased when the reaction temperature increased. The Ni-CS/CNT catalyst prepared

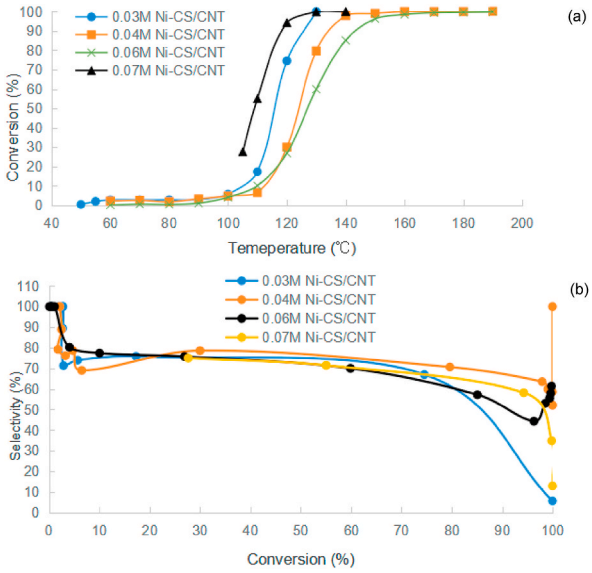

Fig. 6. Acetylene hydrogenation performances on Ni-CS/CNT at different concentrations of $NiSO_4$. (a) acetylene conversion; (b) the relationship between ethylene selectivity and acetylene conversion.

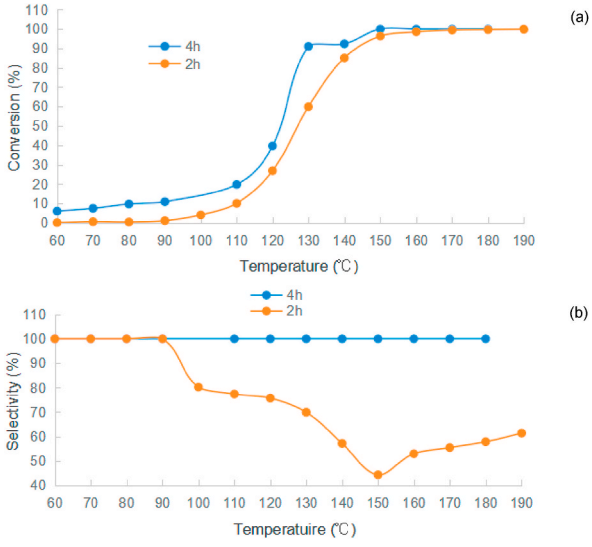

Fig. 7. Effect of CS-CNT crosslinking time on the catalyst performances of Ni-CS/CNT catalysts.

using 1.0 mL glutaraldehyde achieved 100% acetylene conversion at 140 °C; nevertheless, the Ni-CS/CNT catalyst prepared using 0.5 mL glutaraldehyde reached 100% acetylene conversion until 190 °C.

Fig. 8(b) exhibited the selectivity of the Ni-CS/CNT catalysts synthesized using different crosslinking dosages. It can be seen that the selectivity of the Ni-CS/CNT catalyst prepared using 1.0 mL glutaraldehyde always stayed at 100% from 50 °C to 190 °C.

As can be seen that the more the amount of the crosslinker was used, the better the catalytic effect of the resulting Ni-CS/CNT catalyst in the acetylene hydrogenation reaction.

When cross-linking time or the amount of cross-linking agent increased, higher levels of cross-linking reaction would occur. At higher levels of cross-linking, the more extensive three-dimensional network formed. This enhanced the stability of CS in acid solutions and the adsorption ability of CS toward Ni [33]. This might promote that the active Ni was anchored on the surface of CS to induce excellent catalytic performance.

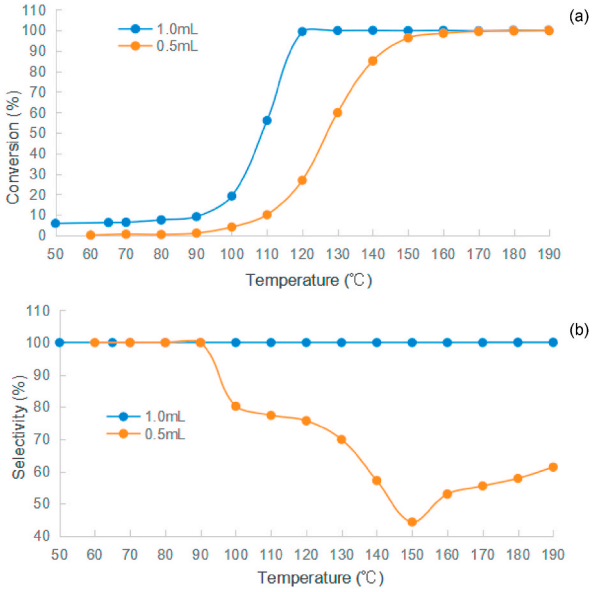

Fig. 8. Effect of crosslinker dosage on the catalytic performances of Ni-CS/CNT.

4. Conclusion

Using biodegradable chitosan, an efficient Ni-based catalyst was prepared for selective hydrogenation of acetylene. The synthesized Ni-CS/CNT catalyst was characterized by ICP, FTIR, SEM and XRD. The results of FTIR and XRD demonstrated that Ni^{2+} successfully coordinated with CS. The addition of CS greatly enhanced the catalytic performances of Ni-CS/CNT due to that the coordination of CS with Ni improved the dispersion of Ni. The catalytic performances of Ni-CS/CNT were even better than Ni single atom catalyst. The catalytic effect of Ni-CS/CNT heightened with the extension of the crosslinking time. The more the amount of the crosslinker was used, the higher the conversion and selectivity of the resulting Ni-CS/CNT catalyst.

Author contribution statement

Siye Tang: Conceived and designed the experiments; Analyzed and interpreted the data; Contributed reagents, materials, analysis tools or data; Wrote the paper.

Liying Li: Conceived and designed the experiments; Contributed reagents, materials.

Xinxiang Cao: Conceived and designed the experiments; Analyzed and interpreted the data; Contributed reagents, materials, analysis tools or data.

Qingqing Yang: Performed the experiments; Analyzed and interpreted the data.

Funding statement

Professor Siye Tang was supported by National Natural Science Foundation of China [21476102].

Xinxiang Cao was supported by Henan Provincial Science and Technology Research Project [212102210214].

Data availability statement

Data included in article/supp. material/referenced in article.

Declaration of interest's statement

The authors declare no competing interests.

References

[1] X.X. Cao, T.T. Lyu, W.T. Xie, A. Mirjalili, A. Bradicich, R. Huitema, B.W. Jang, J.K. Keum, K. More, C.J. Liu, X.L. Yan, Preparation and investigation of Pd doped Cu catalysts for selective hydrogenation of acetylene, Front. Chem. Sci. Eng. 14 (2020) 522–533, https://doi.org/10.1007/s11705-019-1822-3.

[2] A. Borodziński, G.C. Bond, Selective hydrogenation of ethyne in ethene-rich streams on palladium catalysts. Part 1. Effect of changes to the catalyst during reaction. Catalysis reviews: science and engineering, Catal. Rev. 48 (2006) 91–144, https://doi.org/10.1080/01614940500364909.

[3] X.Y. Dai, Z. Chen, T. Yao, L.R. Zheng, Y. Lin, W. Liu, H.X. Ju, J.F. Zhu, X. Hong, S.Q. Wei, Y.E. Wu, Y.D. Li, Single Ni sites distributing on N-doped carbon for selective hydrogenation of acetylene, Chem. Commun. 53 (2017) 11568–11571, https://doi.org/10.1039/C7CC04820C.

[4] H. Liu, M.Q. Chai, G.X. Pei, X.Y. Liu, L. Li, L.L. Kang, A.Q. Wang, T. Zhang, Effect of IB-metal on Ni/SiO_2 catalyst for selective hydrogenation of acetylene, Chin. J. Catal. 41 (2020) 1099–1108, https://doi.org/10.1016/S1872-2067(20)63568-9.

[5] X.X. Cao, A. Mirjalili, J. Wheeler, W. Xie, B.W. Jang, Investigation of the preparation methodologies of Pd-Cu single atom alloy catalysts for selective hydrogenation of acetylene, Front. Chem. Sci. Eng. 9 (2015) 442–449, https://doi.org/10.1007/s11705-015-1547-x.

[6] Y.C. Chai, G.J. Wu, X.Y. Liu, Y.J. Ren, W.L. Dai, C.M. Wang, Z.K. Xie, N.J. Guan, L.D. Li, Acetylene-selective hydrogenation catalyzed by cationic nickel confined in zeolite, J. Am. Chem. Soc. 25 (2019) 9920–9927, https://doi.org/10.1021/jacs.9b03361.

[7] F. Studt, F. Abild-Pedersen, T. Bligaard, R.Z. Sørensen, C.H. Christensen, J.K. Nørskov, Identification of non-precious metal alloy catalysts for selective hydrogenation of acetylene, Science 320 (2008) 1320–1322, https://doi.org/10.1126/science.1156660.

[8] T. Lanza, R. Leardini, M. Minozzi, D. Nanni, P. Spagnolo, G. Zanardi, Approach to spirocyclohexadienimines and corresponding dienones through radical ipso cyclization onto aromatic azides, Angew. Chem. 49 (2008) 9439–9442, https://doi.org/10.1002/anie.200804333.

[9] B. Bridier, J. Pérez-Ramírez, Cooperative effects in ternary Cu−Ni−Fe catalysts lead to enhanced alkene selectivity in alkyne hydrogenation, J. Am. Chem. Soc. 12 (2010) 4321–4327, https://doi.org/10.1021/ja9101997.

[10] A.G. Boudjahem, M. Chettibi, S. Monteverdi, M.M. Bettahar, A.-G. Boudjahem1, M. Chettibi1, S. Monteverdi, M.M. Bettahar, Acetylene hydrogenation over Ni–Cu nanoparticles supported on silica prepared by aqueous hydrazine reduction, J. Nanosci. Nanotechnol. 9 (2009) 3546–3554, https://doi.org/10.1166/jnn.2009.NS28.

[11] Y.A. Liu, J.Y. Zhao, J.T. Feng, Y.F. He, Y.Y. Du, D.Q. Li, Layered double hydroxide-derived Ni-Cu nanoalloy catalysts for semi-hydrogenation of alkynes: improvement of selectivity and anti-coking ability via alloying of Ni and Cu, J. Catal. 359 (2018) 251–260, https://doi.org/10.1016/j.jcat.2018.01.009.

[12] S.A. Nikolaev, V.V. Smirnov, A.Y. Vasil'kov, V.L. Podshibikhin, Synergism of the catalytic effect of nanosized gold-nickel catalysts in the reaction of selective acetylene hydrogenation to ethylene, Kinet. Catal. 51 (2010) 375–379, https://doi.org/10.1134/S0023158410030080.

[13] B. Yang, R. Burch, C. Hardacre, P. Hu, P. Hughes, Selective hydrogenation of acetylene over Cu(211), Ag(211) and Au(211): horiuti–Polanyi mechanism vs. non-Horiuti–Polanyi mechanism, Catal. Sci. Technol. 7 (2017) 1508–1514, https://doi.org/10.1039/C6CY02587K.

[14] B. Yang, R. Burch, C. Hardacre, G. Headdock, P. Hu, Origin of the increase of activity and selectivity of nickel noped by Au, Ag, and Cu for acetylene hydrogenation, ACS Catal. 2 (2012) 1027–1032, https://doi.org/10.1021/cs2006789.

[15] M.Q. Chai, X.Y. Liu, L. Li, G.X. Pei, Y.J. Ren, Y. Su, H.K. Cheng, A.Q. Wang, T. Zhang, SiO_2-supported Au-Ni bimetallic catalyst for the selective hydrogenation of acetylene, Chin. J. Catal. 8 (2017) 1338–1346, https://doi.org/10.1016/S1872-2067(17)62869-9.

[16] G.X. Pei, X.Y. Liu, A.Q. Wang, Y. Su, L. Li, T. Zhang, Selective hydrogenation of acetylene in an ethylene-rich stream over silica supported Ag-Ni bimetallic catalysts, Appl. Catal., A 545 (2017) 90–96, https://doi.org/10.1016/j.apcata.2017.07.041.

[17] B. Talat, I. Tülden, M. Ayfer, Synthesis, characterization, and catalytic activity in Suzuki coupling and catalase-like reactions of new chitosan supported Pd catalyst, Carbohydr. Polym. 145 (2016) 20–29, https://doi.org/10.1016/j.carbpol.2016.03.019.

[18] M. Nasrollahzadeh, N. Shafiei, Z. Nezafat, N.S.S. Bidgoli, F. Soleimani, Recent progresses in the application of cellulose, starch, alginate, gum, pectin, chitin and chitosan based (nano)catalysts in sustainable and selective oxidation reactions: a review, Carbohydr. Polym. 241 (2020) 116353–116376, https://doi.org/10.1016/j.carbpol.2020.116353.

[19] A. Kabirun, S. Gangutri, B. Pakiza, R.G. Sandhya, S. Mitu, T. Hiya, S.I. Nashreen, Selective and green sulfoxidation in water using a new chitosan supported Mo (VI) complex as heterogeneouscatalyst, ChemSelect 3 (2018) 12563–12575, https://doi.org/10.1002/slct.201803000.

[20] T. Baran, A. Mentes, H. Arslan, Synthesis and characterization of water soluble O-carboxymethyl chitosan Schiff bases and Cu(II) complexes, Int. J. Biol. Macromol. 72 (2015) 94–103, https://doi.org/10.1016/j.ijbiomac.2014.07.029.

[21] M.J. Laudenslager, J.D. Schiffman, C.L. Schauer, Carboxymethyl chitosan as a matrix material for platinum, gold, and silver nanoparticles, Biomacromolecules 9 (2008) 2682–2685, https://doi.org/10.1021/bm800835e.

[22] T. Baran, E. Ac¸ıksöz, A. Mentes, Carboxymethyl chitosan Schiff base supported heterogeneous palladium(II) catalysts for Suzuki cross-coupling reaction, J. Mol. Catal. Chem. 407 (2015) 47–52, https://doi.org/10.1016/j.molcata.2015.06.008.

[23] M.A. Abdelkawy, E.A. Aly, M.A. El-Badawi, S. Itsuno, Chitosan-supported cinchona urea: sustainable organocatalyst for asymmetric Michael reaction, Catal. Commun. 146 (2020) 106132–106137, https://doi.org/10.1016/j.catcom.2020.106132.

[24] M.M. Lazar, I.A. Dinu, M. Silion, E.S. Dragan, M.V. Dinu, Could the porous chitosan-based composite materials have a chance to a "NEW LIFE" after Cu(II) ion binding? Int. J. Biol. Macromol. 131 (2019) 134–146, https://doi.org/10.1016/j.ijbiomac.2019.03.055.

[25] T. Baran, A. Menteş, Cu(II) and Pd(II) complexes of water soluble O-carboxymethyl chitosan Schiff bases: synthesis, characterization, Int. J. Biol. Macromol. 79 (2015) 542–554, https://doi.org/10.1016/j.ijbiomac.2015.05.021.

[26] X.Y. Li, K.P. Cui, Z. Guo, T.T. Yang, Y. Cao, Y.P. Xiang, H.H. Chen, M.F. Xi, Heterogeneous Fenton-like degradation of tetracyclines using porous magnetic chitosan microspheres as an efficient catalyst compared with two preparation methods, Chem. Eng. J. 379 (2020) 122324–122337, https://doi.org/10.1016/j.cej.2019.122324.

[27] K. Hasan, I.A. Shehadi, N.D. Al-Bab, A. Elgamouz, Magnetic chitosan-supported silver nanoparticles: a heterogeneous catalyst for the reduction of 4-nitrophenol, Catalysts 9 (2019) 839–856, https://doi.org/10.3390/catal9100839.

[28] Q. Liu, M.D. Xu, Y.D. Wang, R.K. Feng, Z. Yang, S.F. Zuo, C.Z. Qi, M.F. Zeng, Co-immobilization of Pd and Zn nanoparticles in chitosan/silica membranes for efficient, recyclable catalysts used in Ullmann reaction, Int. J. Biol. Macromol. 105 (2017) 575–583, https://doi.org/10.1016/j.ijbiomac.2017.07.081.

[29] G.X. Pei, X.Y. Liu, X.F. Yang, L.L. Zhang, A.Q. Wang, L. Li, H. Wang, X.D. Wang, T. Zhang, Performance of Cu-alloyed Pd single-atom catalyst for semihydrogenation of acetylene under simulated front-end conditions, ACS Catal. 7 (2017) 1491–1500, https://doi.org/10.1021/acscatal.6b03293.

[30] J.H. Advani, N.H. Khan, H.C. Bajaj, A.V. Biradar, Stabilization of palladium nanoparticles on chitosan derived N-doped carbon for hydrogenation of various functional groups, Appl. Surf. Sci. 487 (2019) 1307–1315, https://doi.org/10.1016/j.apsusc.2019.05.057.

[31] M.F. Zeng, X. Zhang, C.Z. Qi, X.M. Zhang, Microstructure-stability relations studies of porous chitosan microspheres supported palladium catalysts, Int. J. Biol. Macromol. 51 (2012) 730–737, https://doi.org/10.1016/j.ijbiomac.2012.07.017.

[32] A.R. Hajipour, P. Abolfathi, Chitosan-supported Ni particles: an efficient nanocatalyst for direct amination of phenols, Appl. Organomet. Chem. 32 (2018) e4273, https://doi.org/10.1002/aoc.4273.

[33] S.L. Sun, A.Q. Wang, Adsorption properties of carboxymethyl-chitosan and cross-linked carboxymethyl-chitosan resin with Cu(II) as template, Separ. Purif. Technol. 49 (2006) 197–204, https://doi.org/10.1016/j.seppur.2005.09.013.